Available online at www.sciencedirect.com
SCIENCE DIRECT®
Sensors and Actuators B 98 (2004) 208–214
SENSORS AND ACTUATORS B CHEMICAL
www.elsevier.com/locate/snb

Poly(dimethylsiloxane) microfluidic flow cells for surface plasmon resonance spectroscopy

Aaron R. Wheeler, Soonwoo Chah, Rebecca J. Whelan, Richard N. Zare*

Department of Chemistry, Stanford University, Stanford, CA 94305-5080, USA

Received 28 May 2003; accepted 10 June 2003

Abstract

A fabrication technique has been developed that uses a novolak-based positive photoresist, SPR-220, for fabrication of channels in poly(dimethylsiloxane) (PDMS) that are up to 61 μm deep. Like methods relying on SU-8 (an epoxy-based negative photoresist), the new method enables rapid design and fabrication of microfluidic devices but avoids possible incompatibilities with standard cleanroom processes. The utility of devices fabricated with this technique is demonstrated for use with surface plasmon resonance spectroscopy (SPR). Two microfabricated flow cells having volumes of 336 and 73 nl were used to detect an analyte in bulk solution and deposition of proteins on a surface.

Keywords: PDMS; Surface plasmon resonance; Microfluidics; Soft lithography; Spreeta; Refractive index

1. Introduction

1.1. Microfluidics

Since microfabricated channels were first used for capillary electrophoresis [1] in the early 1990s, microfluidics has become an increasingly popular technology for chemistry and biology [2,3]. The advantages of microfluidics include reduced scale and reagent use, and the potential for "lab-on-a-chip" integration. Originally, glass was the substrate of choice for microfluidics; however, the arduous efforts required to fabricate such devices have led to the development of alternative fabrication methods using soft materials, such as polymer substrates. One substrate, poly(dimethylsiloxane) (PDMS) [4–14], has been the most popular polymer for microfluidics.

PDMS is widely used because of its compatibility with the rapid fabrication technique of "replica molding" [4–6]. In this technique, PDMS is cast against a positive-relief master, which results in a negative-relief pattern on the surface of the PDMS after curing. Because this process requires only a few hours, fabricating new devices is primarily dependent upon how quickly the masters can be made. Methods for fabricating masters vary considerably, including standard wet etching [7–9] or deep reactive ion etching [10] in silicon, aluminum micromachining [11], or solid object printing [12]. By far the most widely used technique, however, is the process of forming masters directly from thick photoresist patterns [4–6,13,14], known as "soft lithography."

The photoresist used for the majority of soft lithography methods is the photocurable epoxy SU-8 (MicroChem Corp., Newton, MA) [4–6]. SU-8 is a negative resist that can be deposited at thicknesses up to 200 μm. It does not suffer from swelling like other negative resists, and it can be used to pattern features with very high aspect ratios [15]. Unfortunately, it adheres strongly to many substrates, and very few solvents can strip cured SU-8 [15]. Thus, SU-8 is sometimes forbidden for use in cleanroom processing equipment that has not been dedicated for use with epoxy photoresists.

Regnier and coworkers [13,14] have demonstrated the use of a different photoresist, SPR-220 (Shipley Microelectronics, Marlborough, MA), to make masters with features that are 10 μm tall for soft lithography. In contrast to SU-8, SPR-220 is a standard novolak resin-based positive photoresist, which is compatible with all conventional photolithographic processes. In the present work, SPR-220[1] was used to make masters with features from 16 to 61 μm tall. As far as we are aware, the microfluidic devices formed from these masters are the deepest channels ever created using a positive photoresist for soft lithography. It is anticipated

* Corresponding author. Tel.: +1-650-723-3062; fax: +1-650-725-0259.
E-mail address: zare@stanford.edu (R.N. Zare).

[1] The abbreviation for surface plasmon resonance, SPR, and the photoresist used for soft lithography, SPR-220, are not related.

0925-4005/$ – see front matter © 2003 Elsevier B.V. All rights reserved.
doi:10.1016/j.snb.2003.06.004

that this method may be useful for those who do not have access to equipment compatible with epoxy-based negative photoresists.

The novel soft lithography fabrication method presented in this work was developed in response to Stanford Nanofabrication Facility (SNF) restrictions on the use of SU-8. It is anticipated that this new method will be useful as a complementary tool to SU-8-based soft lithography methods for those who face similar restrictions. Microfluidic flow cells fabricated using the new technique were demonstrated for use with surface plasmon resonance spectroscopy (SPR).

1.2. Surface plasmon resonance spectroscopy

The principles of SPR[1] have been explained in detail elsewhere [16,17]; for the purposes of this work, it is enough to know that SPR is a phenomenon that enables label-free detection of analytes based on their refractive indices (RI). The SPR signal is strongest when measuring RI near the surface of a sensor; thus, it is often used to detect surface binding characteristics of biomolecules [17].

To increase the availability of analytes at a sensor's surface, SPR is often used in conjunction with flowing streams of analytes. This technique often requires prohibitive use of large volumes of expensive reagents; to avoid this problem, techniques have been developed to limit the detection volume. The BIAcore system (Biacore AB, Uppsala, Sweden) [18–20], which has been commercially available for the last decade, utilizes a microfluidic flow chamber that encloses (including dead volume) a few hundred nanoliters [20]. Others [21–24] have used microfluidic flow cells coupled to table-top SPR setups, requiring lasers, detectors, and rotation stages. Each of these options requires a fairly large laboratory "footprint."

A third option for SPR is the Spreeta (Texas Instruments, Dallas, TX) [25,26]. This device is approximately 40 mm × 40 mm × 15 mm and thus requires a comparatively small footprint to the other options for SPR. Unfortunately, the Spreeta is equipped with a relatively large flow cell (8 μl, including dead volume [27]), which increases the reagent consumption for analysis of flowing analytes. In response to this problem, we [28,29] have previously employed smaller flow cells (3.5 μl and 400 nl) for use with the Spreeta SPR detector. The present work is an extension of these efforts—we have combined the Spreeta detector with microfabricated flow cells formed from PDMS.

Chinowsky et al. [30] has recently reported the development of a second generation Spreeta, the "Spreeta 2000." In describing the operation of the device, Chinowsky et al. mention use of a 100-nl flow cell; however, no description of the fabrication method or materials is reported. In the present work, the methodological details, materials, and dimensions of an easy-to-fabricate PDMS flow cell for use with the Spreeta SPR detector is reported. SPR is merely an example; we anticipate that the new fabrication method may be useful for a variety of techniques that would benefit from the use of low-volume flow cells.

2. Experimental

2.1. Materials

All chemicals were purchased from Sigma (St. Louis, MO) and used without modification unless otherwise noted. RTV 615 PDMS was from GE Silicones (Waterford, NY). Shipley Microelectronics SPR-220 photoresist and LDD-26W developer were purchased from MicroChem Corp. (Newton, MA). Stock solutions of sodium borate (100 mM boric acid) were prepared from deionized water and brought to pH 9 with sodium hydroxide. Benzyl alcohol solutions were prepared in borate buffer. Biotinylated bovine serum albumin (B-BSA), streptavidin, and biotinylated protein A were purchased from Pierce (Rockford, IL), reconstituted, aliquotted, and stored according to the vendor's instructions. Prior to use, B-BSA (20 μg/ml), streptavidin (50 μg/ml), biotinylated protein A (10 μg/ml), and human IgG (100 μg/ml) were diluted into Dulbecco's phosphate buffered saline (PBS) purchased from Invitrogen (Carlsbad, CA).

2.2. Microfluidic device fabrication

Reusable masters for soft lithography were constructed from patterns of photoresist on silicon using standard microlithography techniques at SNF. Briefly, silicon wafers were silanized with hexamethyldisilazane (HMDS) and spin coated with SPR-220 photoresist (1000 RPM, 40 s). Up to three coats of SPR-220 were applied to achieve greater thicknesses; between each step, the wafers were baked on a hotplate (90 °C, 60 s). After the final coat, the wafers were postbaked in two steps, on a hotplate followed by being placed in an oven (face up). The spin coating and postbake conditions, along with the final feature thicknesses, are found in Table 1. After coating and baking, wafers were left to sit overnight before processing.

Wafers were exposed (16 mW/cm^2) through transparency film masks in soft contact mode, in intervals. The exposure times for different photoresist thicknesses can be found in Table 1. After exposure, wafers were immersed in LDD-26W developer and agitated until development (confirmed visually). The dimensions of the photopatterned features were measured with profilometry. The photopatterned lines were

Table 1
Master fabrication parameters

Channel depth (μm)	# Coats	Hotplate (°C s)	Oven (°C min)	Exposure time (s)
16	1	90, 60	90, 55	2 × 30
39	2	90, 120	90, 75	4 × 30
61	3	90, 180	90, 90	5 × 40

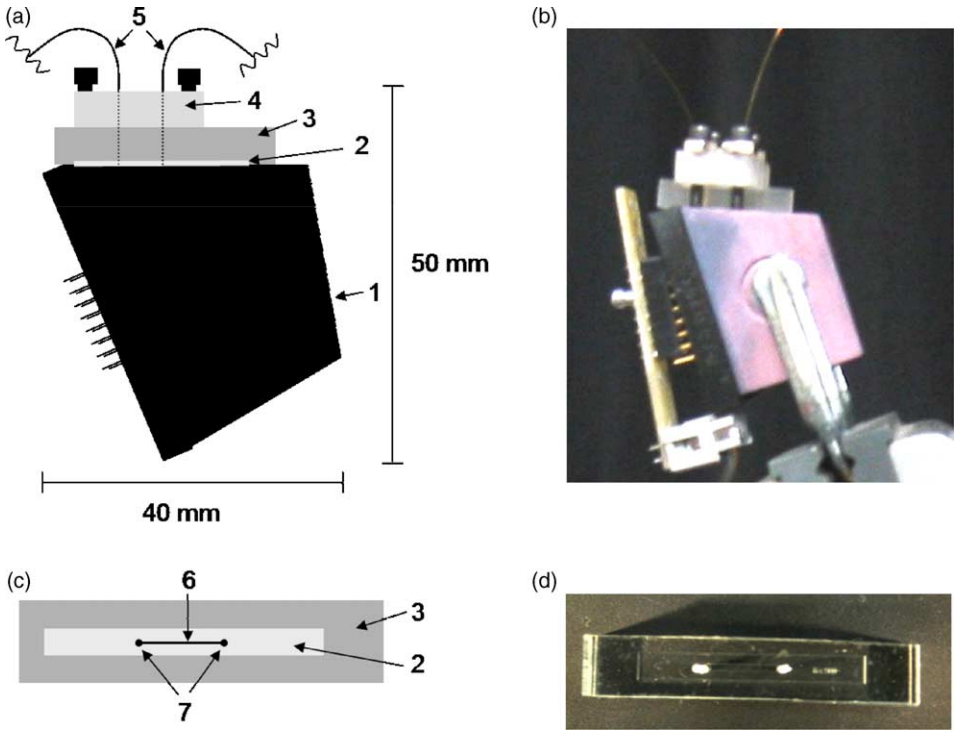

Fig. 1. Schematics (a and c) and pictures (b and d) of Spreeta with microfabricated flow cell. Spreeta, 1; gold sensing surface, 2; PDMS flow cell, 3; clamp, 4; inlet and outlet capillaries, 5; microfluidic channel, 6; inlet/outlet holes, 7.

roughly trapezoidal: the "top" of each feature was often ~20% more narrow than the "base."

Fluidic devices were prepared from RTV 615 PDMS using soft lithography [4–6,13,14]. Briefly, base and curing agent were mixed (10:1, by weight) and then degassed in an evacuated chamber (~100 Torr, 1 h). A master was silanized with trimethyl chlorosilane (TMCS) vapor (5 min), and then PDMS was poured onto it. After curing (80 °C in an oven for 3 h), the PDMS slab was peeled from the master, trimmed, and inlet holes were punched with a blunt 25-gauge needle (Small Parts, Inc., Miami Lakes, FL). The finished product (not attached to the Spreeta) was ~5 mm × 25 mm × 5 mm.

2.3. Experimental set-up

The PDMS flow cells were trimmed to fit onto the Spreeta's gold surface (see Fig. 1). Each flow cell had a single 6 mm long channel running down the center of the device; the channel was designed and aligned to enclose the active region of the sensor. Three different channel widths were fabricated: 200, 500, and 1000 μm. Versions of each device were created with three different depths: 16, 39, and 61 μm. As far as we are aware, this is the first example of using a conventional positive photoresist to create "deep" microfluidic channels (>10 μm) using soft lithography. All data shown in this work were collected with the 61 μm deep channels, with widths of 1000 or 200 μm (366 or 73 nl, respectively; these volumes are approximate, given the nonrectangular profile).

SPR measurements were performed using a Spreeta sensor (Texas Instruments, Dallas, TX). The combined apparatus (PDMS flow cell and sensor) was held together with a custom-machined clamp, and tightened with screws (see Fig. 1). The combined apparatus was approximately 50 mm × 40 mm × 15 mm—a very small laboratory footprint.

Flow through the cells was driven with pressure from a Harvard Apparatus Model 11 Syringe Pump (Holliston, MA), mated to a fused silica capillary (50 cm, 360 μm o.d., 150 μm i.d., Polymicro Technologies, Phoenix, AZ). To seal the capillary into the flow cell inlet, stainless steel 25 gauge sleeves were affixed with glue encircling the capillary outlet. Refractive Index data was collected at 1.2 Hz and recorded and collected into a PC. Data was plotted as a function of time using LabView software (National Instruments, Austin, TX). For protein immobilization studies, a two-position, six-port Cheminert switching valve (VICI, Houston, TX) was used.

As a reference for characterizing the microfluidic flow cells, the performance of a 3.5 μl flow cell [28,29] was also evaluated.

2.4. Experimental procedure

Prior to use, and between runs, the Spreeta's gold surface was cleaned by gently wiping with a cotton swab or Kimwipe soaked in 1% sodium dodecyl sulfate solution followed by rinsing with distilled water. The surface was allowed to dry in air. PDMS flow cells were cleaned with methanol and

clamped onto the sensor. Capillaries were then inserted into the inlet holes, and methanol (followed by aqueous buffers) was pumped through the flow cell until stable SPR signal was observed. It is well known that wetting and filling PDMS microchannels without air bubbles is a challenge because of the hydrophobic walls. This challenge was overcome in these experiments by wetting the channels with methanol prior to using aqueous solutions (as has been previously reported [8]).

In order to avoid leaks, the flow cells had to be clamped tightly, which sometimes collapsed the "shallow" (16 μm deep) channels. Under these conditions, stable SPR signal could only be achieved by pumping at high flow rates (∼ml/h). The channels with larger aspect ratios of depth to width (39 or 61 μm) were observed not to suffer from this problem. When using these flow cells, flow rates as low as 20 μl/h were feasible without leaking or channel collapse. All data shown was collected with the 61 μm deep channels.

For peak detection experiments, plugs of benzyl alcohol (0.4% in 100 mM borate buffer, pH 9) were introduced into the column inlet by hydrodynamic injection (30 cm, 10 s) [31]. The capillary was then mated to the syringe pump, and the plug was pushed toward the detector at one of four flow rates: 1 ml/h, 500, 100, and 50 μl/h. For each flow cell and flow rate, at least three replicate injections were made. Data were processed with Igor Pro software (Wavemetrics, Lake Oswego, OR). Data were first Fast Fourier Transform (FFT) notch filtered to remove periodic noise caused by the syringe pump, and then smoothed with a running average (every five points). This procedure was observed not to affect peak heights, shapes, or widths. Data were then baseline subtracted and normalized, and a variety of parameters were calculated including area, variance, and skew, using home-written code based on "statistical moments" [32]. Peak width, defined as six times the square root of the variance, was also calculated.

For protein deposition experiments, the syringe pump pushed PBS to the Spreeta through polyethylene tubing. After stable SPR signal was established, protein solutions in PBS were loaded sequentially into a 100-μl sample loop on the switching valve, and then injected into the flow stream. During the protein layering steps, the solution flow rate was 1.2 ml/h, such that each protein solution was in contact with the gold SPR surface for 5 min. The 200 μm × 61 μm flow cell (73 nl) was used for these experiments.

3. Results and discussion

The flow cells were fabricated with soft lithography as described in Section 2.2. Fabrication of the master required parts of two days' work in the cleanroom. Fabrication of a batch of flow cells (from one master) required a few hours; each master was used multiple times to create many batches. With the present device, 20 flow cells were formed from each batch; it is estimated that a more efficient use of the design on the master might yield >100 flow cells per batch. Additionally, it was straightforward for one experimenter to create 2–3 batches simultaneously. Clearly, this method is appropriate for high volume fabrication of flow cells for use with chemical sensing.

Surface plasmon resonance was used as a model technique to characterize the utility of the flow cells. Two methods were tested: detection of injections in bulk solution, and detection of binding of sequential layers of protein.

3.1. Injections in bulk solution

This work was motivated by efforts to use the Spreeta as a detector for separations such as capillary electrophoresis (CE) [29]. For such applications, a "plug" of sample is injected into the inlet of a separation column and then detected near the outlet of the column. In these experiments, to mimic chromatographic peaks, hydrodynamic injections of benzyl alcohol were pushed with a syringe pump through a capillary attached to the flow cell. As eluent moved through the flow chamber, refractive index was plotted as a function of time to mimic a chromatogram. Typical results for four flow rates, using a home-built 3.5 flow cell, are found in Fig. 2.

It is apparent from Fig. 2 that peaks injected and detected in this manner are not ideal for chromatography. At the faster flow rates (1 ml/h and 500 μl/h), the detector responds too slowly to measure the full refractive index change. At the slower flow rates (100 and 50 μl/h), the peaks show considerable tailing, and are extremely broad. These slower flow rates (which translate to linear velocities in the capillary of 1.57 and 0.78 mm/s, respectively) are particularly important because they are "typical" velocities for CE. A primary reason for this peak broadening is the mismatch in cross-sectional areas (X-A) between the capillary and the flow cell (see Table 2). Although the volumetric flow rate is constant between the column and the flow cell, the linear velocity (proportional to X-A) is not. In this case, the velocity in the flow cell is expected to be ∼3% of the velocity in the capillary. As the injected plug leaves the faster moving solution in the capillary and spreads into the slower moving solution in the flow cell, the peak broadens. As

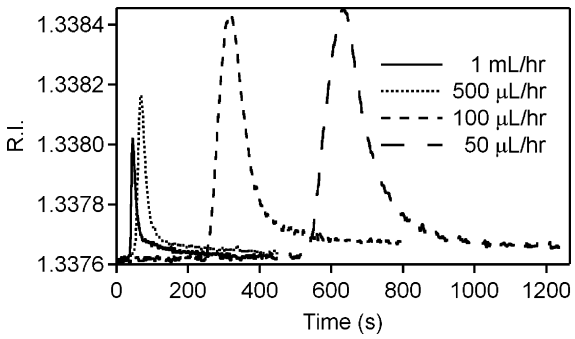

Fig. 2. Four injections of 0.4% benzyl alcohol at four different flow rates with a 3.5-μl flow cell.

Table 2
Flow cell dimensions

Device	Length (mm)	Width (μm)	Depth (μm)	Volume (nl)	X-A (μm^2)
Capillary	–	–	–	–	17671
Macro-flow cell	6	1500	390	3510	585000
Micro-flow cell	6	1000	61	366	61000
Micro-flow cell	6	200	61	73.2	12200

shown in Fig. 2, this is especially apparent at slower flow rates.

With this in mind, PDMS microfluidic flow cells were developed for use with the Spreeta detector. Two flow cells were used; Table 2 summarizes their dimensions. Hydrodynamic injections of benzyl alcohol were used to characterize these flow cells. As with the 3.5-μl flow cell, refractive index change responses were collected for a variety of flow rates. A comparison of peak shapes for the 100 μl/h flow rate is depicted in Fig. 3. The differences are obvious; the width of the peak generated with the 3.5-μl flow cell is much larger than that of the microfluidic flow cells. This was true for all flow rates, as summarized in Fig. 4. Interestingly, the peak tailing, observed graphically in Fig. 3, and quantified by skew >0 (data not shown) was best for the 366-nl flow cell, but the skew of peaks generated with the 73-nl flow cell was similar to that from the 3.5-μl flow cell.

Fig. 3 makes it clear that selecting columns and flow cells with matching X-A is important for these kinds of applications. It should be noted that the design and fabrication method described in Section 2.2 is very easy; many different flow cells with many different dimensions can be fabricated rapidly to match the X-A's of a variety of columns.

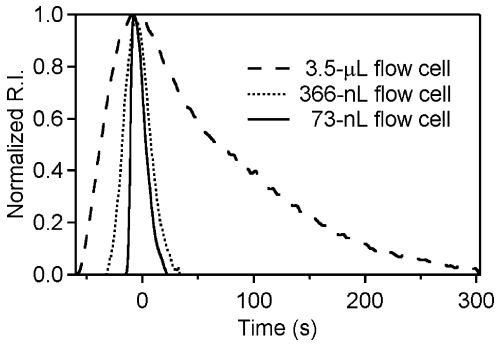

Fig. 3. Three injections of 0.4% benzyl alcohol at 100 μl/h into three different flow cells: 3.5 μl, 366 and 73.2 nl. Only the peaks are shown; they have been normalized and offset horizontally such that the center of each peak was positioned at $t = 0$.

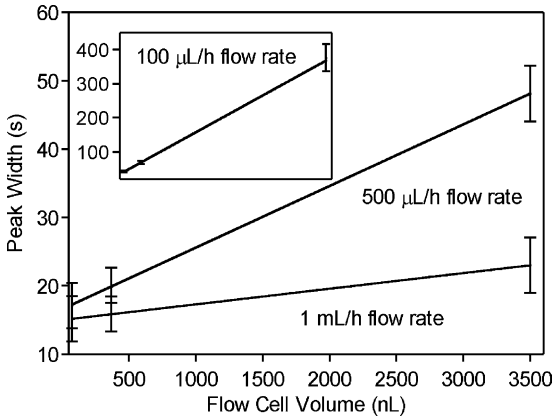

Fig. 4. Peak width as a function of flow cell volume. Error bars are ±1S.D. Each point represents at least three replicate measurements.

3.2. Protein deposition

Although comparing the detection of plugs of bulk solution is useful to characterize the performance of the devices, SPR is most often used to characterize chemical dynamics on surfaces, such as protein binding. In the present work, microfluidic PDMS flow cells were used to enable SPR detection of a four-step protein binding assay, represented schematically in Fig. 5. Biotinylated bovine serum albumin (B-BSA), which nonspecifically adhered to the gold surface, was deposited first. B-BSA was followed by successive depositions of streptavidin, biotinylated protein A, and human IgG, all of which bound specifically to the preceding layer. As these solutions flowed through the device, refractive index was plotted as a function of time, as can be seen in Fig. 6.

A change in refractive index was observed with the binding of each protein: B−BSA, 6.25×10^{-4}, streptavidin, 3.44×10^{-3}, protein A, 4.76×10^{-4}, IgG, 2.07×10^{-3}. This agrees well with data we collected previously using a larger flow cell [29]. One expected challenge was nonspecific adsorption of proteins [33] to the hydrophobic surface of the PDMS flow chamber. With the high protein concentrations used, this was not an issue; however, at low concentrations and flow rates, the amount of protein binding to the PDMS may compete with the binding to the gold SPR surface. In these cases, the PDMS could be pretreated with BSA [33] to prevent protein adsorption.

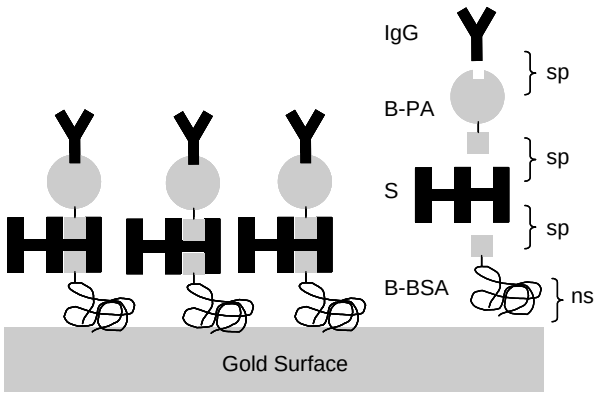

Fig. 5. Schematic of deposition of layers of biotinylated BSA (B-BSA), streptavidin (S), biotinylated Protein A (B-PA), and IgG (IgG). The first binding event is nonspecific adsorption (ns); the other events are specific molecular recognition (sp).

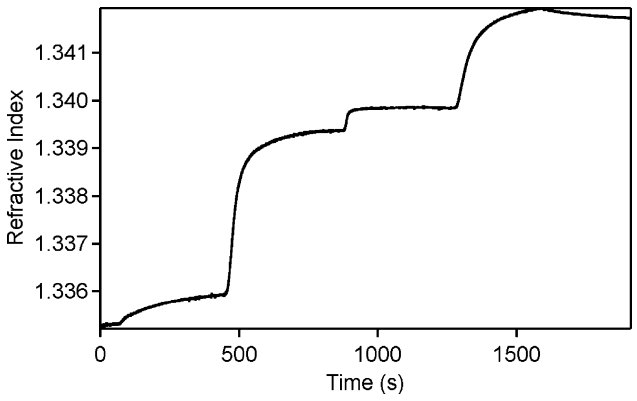

Fig. 6. Sensorgram of biotinylated BSA, streptavidin, biotinylated Protein A, and human IgG. Solutions in PBS were pushed through a 73.2-nl flow cell at 1.2 ml/h.

4. Conclusion

A new soft lithography fabrication method is reported for making microchannels up to 61 μm deep in PDMS. Like other soft lithography methods, the new method was straightforward and fast, which enabled rapid prototyping of a microfluidic design. Unlike other methods, which use an epoxy-based negative photoresist, the new method uses a standard novolak resin-based positive photoresist. This method should be useful for those who do not have access to equipment compatible with epoxy-based resists.

Devices formed in this manner were demonstrated for use with surface plasmon resonance spectroscopy. For detection of injected plugs of benzyl alcohol, the microfluidic flow cells generated peaks that were much thinner than those generated with a macroscale flow cell. These data highlight the importance of matching the cross-sectional area of the flow cell to that of the delivery column. The microfluidic devices were also used for a conventional SPR function: to enable detection of sequential layers of protein binding.

This rapid, simple fabrication method should be useful for those who require low volumes for SPR, or for any of a variety of other methods requiring small volume fluid handling.

Acknowledgements

SWC was supported by a Post-doctoral Fellowship from the Korea Science & Engineering Program Foundadtion (KOSEF).

References

[1] A. Manz, D.J. Harrison, E.M.J. Verpoorte, J.C. Fettinger, A. Paulus, H. Ludi, H.M. Widmer, Planar chips technology for miniaturization and integration of separation techniques into monitoring systems: capillary electrophoresis on a chip, J. Chromatogr. 593 (1992) 253–258.

[2] D.R. Reyes, D. Iossifidis, P.A. Auroux, A. Manz, Micro total analysis systems. 1. Introduction, theory, and technology, Anal. Chem. 74 (2002) 2623–2636.

[3] S.C. Jakeway, A.J. De Mello, E.L. Russell, Miniaturized total analysis systems for biologcial analysis, Fresenius. J. Anal. Chem. 366 (2000) 525–539.

[4] D.C. Duffy, J.C. McDonald, O.J.A. Schueller, G.M. Whitesides, Rapid prototyping of microfluidic systems in poly(dimethylsiloxane), Anal. Chem. 70 (1998) 4974–4984.

[5] J.C. McDonald, D.C. Duffy, J.R. Anderson, D.T. Chiu, H. Wu, O.J.A. Schueller, G.M. Whitesides, Fabrication of microfluidic systems in poly(dimethylsiloxane), Electrophoresis 21 (2000) 27–40.

[6] J.C. McDonald, G.M. Whitesides, Poly(dimethylsiloxane) as a material for fabricating microfluidic devices, Acc. Chem. Res. 35 (2002) 491–499.

[7] C.S. Effenhauser, G.J.M. Bruin, A. Paulus, M. Ehrat, Integrated Capillary Electrophoresis on Flexible Silicone Microdevices: Analysis of DNA Restriction Fragments and Detection of Single DNA Molecules on Microchips, Anal. Chem. 69 (1997) 3451–3457.

[8] G. Ocvirk, M. Munroe, T. Tang, R. Oleschuk, K. Westra, D.J. Harrison, Electrokinetic control of fluid flow in native poly(dimethylsiloxane) capillary electrophoresis devices, Electrophoresis 21 (2000) 107–115.

[9] X. Ren, M. Bachman, C. Sims, G.P. Li, N. Allbritton, Electroosmotic properties of microfluidic channels composed of poly(dimethylsiloxane), J. Chromatogr. B. 762 (2001) 117–125.

[10] A. Bernard, B. Michel, E. Delamarche, Micromosaic Immunoassays, Anal. Chem. 73 (2001) 8–12.

[11] B.D. DeBusschere, G.T.A. Kovacs, Portable cell-based biosensor system using integrated CMOS cell-cartridges, Biosens. Bioelectron. 16 (2001) 543–556.

[12] J.C. McDonald, M.L. Chabinyc, S.J. Metallo, J.R. Anderson, A.D. Stroock, G.M. Whitesides, Prototyping of microfluidic devices in poly(dimethylsiloxane) using solid-object printing, Anal. Chem. 74 (2002) 1537–1545.

[13] B.E. Slentz, N.A. Penner, E. Lugowska, F. Regnier, Nanoliter capillary electrochromatography columns based on collocated monolithic support structures molded in poly(dimethyl siloxane), Electrophoresis 2001 (2001) 3736–3743.

[14] B.E. Slentz, N.A. Penner, F. Regnier, Sampling BIAS at channel junctions in gated flow injections on chips, Anal. Chem. 74 (2002) 4835–4840.

[15] J.M. Shaw, J.D. Gelorme, N.C. LaBianca, W.E. Conley, S.J. Holmes, Negative photoresists for optical lithography, IBM J. Res. Dev. 41 (1997) 81–94.

[16] J. Homola, S.S. Yee, G. Gauglitz, Surface plasmon resonance sensors: review, Sens. Actuators B 54 (1999) 3–15.

[17] R.J. Green, R.A. Frazier, K.M. Shakesheff, M.C. Davies, C.J. Roberts, S.J.B. Tendler, Surface plasmon resonance analysis of dynamic biological interactions with biomaterials, Biomaterials 21 (2000) 1823–1835.

[18] M. Malmqvist, Biospecific interaction analysis using biosensor technology, Nature 361 (1993) 186–187.

[19] U. Jonsson, L. Fagerstam, R. Ivarsson, B. Johnsson, R. Karlsson, K. Lundh, S. Lofas, B. Persson, H. Roos, I. Ronnberg, S. Sjolander, E. Stenberg, R. Stahlberg, C. Urbaniczky, H. Ostlin, M. Malmqvist, Real-time biospecific interaction analysis using surface plasmon resonance and a sensor chip technology, Biotechniques 11 (1991) 620–627.

[20] S. Sjolander, C. Urbaniczky, Integrated fluid handling system for biomolecular interaction analysis, Anal. Chem. 63 (1991) 2338–2345.

[21] H.J. Lee, T.T. Goodrich, R.M. Corn, SPR imaging measurements of 1-D and 2-D DNA microarrays created from microfluidic channels on gold thin films, Anal. Chem. 71 (2001) 5525–5531.

[22] M. Furuki, J. Kameoka, H.C. Craighead, M.S. Isaacson, Surface plasmon resonance sensors utilizing microfabricated channels, Sens. Actuators B 79 (2001) 63–69.

[23] M.J. O'Brien, V.H. Perez-Luna, S.R.J. Brueck, G.P. Lopez, A surface plasmon resonance array biosensor based on spectroscopic imaging, Biosens. Bioelectron. 16 (2001) 97–108.
[24] R.A. Vijayendran, K.M. Motsegood, D.J. Beebe, D.E. Leckband, Evaluation of a three-dimensional micromixer in a surace-based biosensor, Langmuir 19 (2003) 1824–1828.
[25] J. Melendez, R. Carr, D. Bartholomew, H. Taneja, S. Yee, C. Jung, C. Furlong, Development of a surface plasmon resonance detector for commercial applications, Sens. Actuators B 38–39 (1997) 375–379.
[26] J.L. Elkind, D.I. Stimpson, A.A. Strong, D.U. Bartholomew, J.L. Melendez, Integrated analytical sensors: the use of the TISPR-1 as a biosensor, Sens. Actuators B 54 (1999) 182–190.
[27] Nomadics, Inc. http://aigproducts.com/surface_plasmon_resonance/spr_flow_cell.htm.
[28] R.J. Whelan, T. Wohland, L. Neumann, B. Huang, B.K. Kobilka, R.N. Zare, Analysis of biomolecular interactions using a miniaturized surface plasmon resonance sensor, Anal. Chem. 74 (2002) 4570–4576.
[29] R.J. Whelan, R.N. Zare, Surface plasmon resonance detection for capillary electrophoresis separations, Anal. Chem. 75 (2003) 1542–1547.
[30] T.M. Chinowsky, J.G. Quinn, D.U. Bartholomew, R. Kaiser, J.L. Elkind, Performance of the Spreeta 2000 integrated surface plasmon resonance affinity sensor, Sens. Actuators B 91 (2003) 266–274.
[31] D.R. Baker, Capillary Electrophoresis, Wiley, New York, NY, 1995, pp. 96–100.
[32] E. Grushka, M.N. Myers, P.D. Schettler, J.C. Giddings, Computer characterization of chromatographic peaks by plate height and higher central moments, Anal. Chem. 41 (1969) 889–892.
[33] E. Ostuni, C.S. Chen, D.E. Ingber, G.M. Whitesides, Selective deposition of proteins and cells in arrays of microwells, Langmuir 17 (2001) 2828–2834.